

# Perception of non-native phoneme contrasts in 8-13 months infants: tensor-based analysis of EEG signals

Mansoureh Aghabeig<sup>1,2</sup>, Bibiana Bałaj<sup>3</sup>, Joanna Dreszer<sup>3</sup>, Monika Lewandowska<sup>3</sup>, Rafał Milner<sup>4</sup>, Natalia Pawlaczyk<sup>5</sup>, Tomasz Piotrowski<sup>1,2</sup>, Magdalena Szmytke<sup>6</sup> and Włodzisław Duch<sup>1,2</sup>

<sup>1</sup>Neurocognitive Laboratory, Center for Modern Interdisciplinary Technologies, Nicolaus Copernicus University, Poland

<sup>2</sup>Dept. of Informatics, Faculty of Physics, Astronomy & Informatics, Nicolaus Copernicus University, Poland  
Email: m.aghabeig@fizyka.umk.pl

<sup>3</sup>Dept. of Psychology, Faculty of Humanities, Nicolaus Copernicus University, Poland

<sup>4</sup>Dept. of Experimental Audiology, World Hearing Center, Institute of Physiology and Pathology of Hearing, Poland

<sup>5</sup>Dept. of Neuropsychology, Faculty of Psychology, University of Warsaw, Poland

<sup>6</sup>Institute of Psychology, Faculty of Educational Sciences, University of Lodz, Poland

**Abstract**—Result of analysis of EEG responses of infants between 8-13 months of age to the syllable speech sounds are presented. We conducted an ERP experiment with an oddball paradigm consisting of two types of deviant stimuli (easy and hard) and standard stimulus. A nonnegative Tucker tensor decomposition (NTD) was used to characterize differences in processing of stimuli using a time-frequency-spatial (multi-domain) features. We extracted the multi-domain features for a reliable representation of the underlying infant brain activity to analyze the processing of standard and deviant stimuli. The obtained results show significant differences in processing between standard and deviant stimuli and may be interpreted in terms of mismatch negativity (MMN) and acoustic change complex (ACC) evoked potentials. Moreover, these results serve as a proof-of-concept for application of tensor decomposition-based analyses for challenging infant EEG data.

**Index Terms**—infant EEG, event-related potentials, time-frequency-spatial features, nonnegative Tucker tensor decomposition

## I. INTRODUCTION

The early development of speech perception skills of infants that constitute a foundation for future learning of language has not been fully understood. The Mismatch Negativity (MMN) is a component of an event-related potential (ERP) typically elicited in response to rare stimuli (deviants) presented in a series of frequent ones (standards) during a passive oddball paradigm [1]. The MMN is an indicator of detection of the acoustic change in a sequence of frequent sounds [1]. It occurs regardless of whether a subject is paying attention to the sequence, which makes it very useful for testing how newborns and infants discriminate speech sounds [2]. The source of MMN signal is located in the auditory cortex and in the frontal lobe [3]. Similarly to the MMN, the Acoustic Change Complex (ACC) that is obtained in response to a stimulus that contains multiple time-varying acoustic changes [4] reflects discrimination capacity in the absence of attention. Its generator is located in the auditory cortex. However, it is much larger in amplitude and requires much fewer stimulus presentations than the MMN. ACC is used for evaluation of speech sound discrimination and perception in clinical applications [5]. Considering that a signal to noise ratio is

usually very low in infant EEG data, we expect that ACC response will be more robust and consistent than MMN in infants EEG signal.

In our study, we have used a passive oddball paradigm with two types of deviant syllables and one standard syllable from a language that is foreign to the child. Averaging the data across epochs separately for each stimulus type showed that the time window containing the MMN component is in [500, 700] ms interval after stimulus onset for all subjects. In response to both types of deviant syllables and standards ACC-like P1-N1-P2-N2 complex is observed. Thus, it is quite likely that for infant data characterized by a low signal-to-noise ratio the MMN and ACC responses overlap. This implies that it is not possible to determine whether ACC contributes to the MMN using a conventional ERP analysis that provides information about ERP component features only in the time domain.

On the other hand, factorization-based approaches are widely used in analysis of EEG signals [6]– [7]. In particular, tensor decomposition methods allow to investigate not only temporal but also spatial and frequency characteristics simultaneously [8]. They also provide a good framework for the group-level analysis of ERP [9]– [10]. There are two traditional models for tensor decomposition: Canonical Polyadic Decomposition (CPD) and Tucker Decomposition (TD) [11] [12]. In this study we chose TD, as this decomposition allows more flexibility to choose components from factor matrices compared with CPD, and it has also been shown in [10] that TD is more robust to low signal-to-noise ratio than CPD. This is especially important in our settings as the infant EEG data is inherently noisy. Furthermore, we incorporated nonnegativity constraints on the TD (NTD) as the time-frequency (power spectrum) representation (TFR) of the EEG signal can attain only nonnegative values. The multi-domain features extracted using tensor decomposition may be used to differentiate across groups using tests for statistical significance. Indeed, such multi-domain features convey more information and yield better insight into data than single domain analysis, offering a better representation of cognitive functions. [9] [10]. They

This work was supported by a grant from the Polish National Science Centre (DEC-2013/08/W/HS6/00333).

can be also used to train a classifier for diagnosis of brain disorders [13] [8].

In this paper, we focus on statistical testing approach, where the main goal of this study is to extract a desired multi-domain feature from infant EEG data using NTD clearly representing the MMN component occurring in the [500, 700] ms time window. In particular, an analysis using tensor decomposition allows us to characterize this component in time-, frequency-, and space- domains simultaneously, and to determine whether the ACC contributes to the MMN component.

## II. METHOD

### A. Data acquisition and preprocessing

Acquiring infant EEG is very difficult due to the large number of artifacts related to movement. The data of 21 healthy native Polish infants (10 boys, mean age = 10 months, SD = 1.3 months, age range: 8.5-12.8 months) was collected in the BabyLab at the Nicolaus Copernicus University.

Infants participated in the passive oddball paradigm consisting of two deviants, called easy and hard, and a standard stimulus. French syllables of 350 ms duration were used as stimuli, recorded in a soundproof chamber by a professional native male speaker. Spectral characteristics of the stimuli were analyzed using Praat software system [14] and are shown in Fig.1. The deviant syllables were chosen from those which were categorized by adult Polish native speakers, not familiar with French, as either easy (easy) or difficult (hard) to discriminate from the standard syllable.

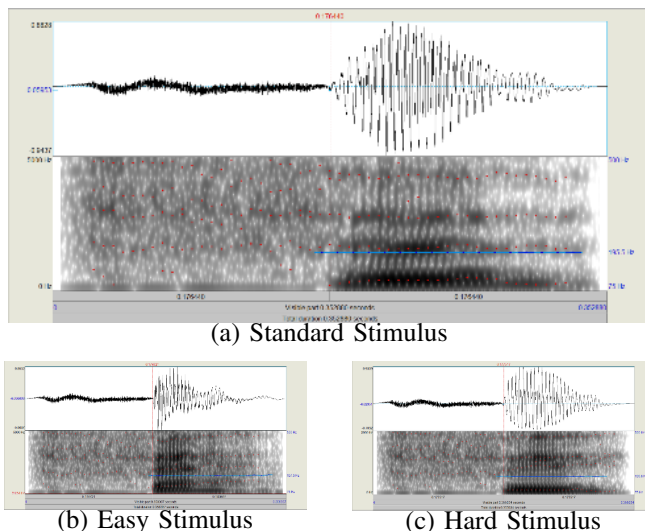


Fig. 1. Spectral characteristics of the stimuli used in the experiment.

The inter-trial-interval was 800 ms plus a jitter following exponential distribution with an expected value of 100 ms, truncated to fit the maximum trial interval length (1000 ms after stimulus onset). The random variable for the number of standard stimuli preceding a deviant stimulus followed a geometric distribution with success probability 1/3. For this random variable, "failures" were the occurrences of standard stimulus, and "successes" were the occurrences of deviant

stimuli. This implies that on average there were 75% of standard stimulus and 25% of deviant stimuli presented during the experiment. Another random variable following Bernoulli distribution with  $p = 1/2$  was used to determine which deviant stimulus should be presented, yielding that, on average, 12.5% of both "easy" and "hard" deviants have been presented during the experiment. The choice of exponential distribution for jitter, and geometric distribution for the number of standards before deviant, was made to take advantage of their memoryless property, implying that infants were less likely to adapt to certain patterns of time intervals between subsequent trials, and to the sequence of trials, respectively. This is especially important considering the overall shortness of inter-trial-intervals (900 ms on average) which was necessary to record sufficiently large number of trials for an infant.

A child was seated on caregivers lap in front of the monitor at a distance of 1 m. During the EEG data recording silent cartoons were shown on the monitor. A caregiver was asked to sit without talking and to refrain interacting with a child. The stimuli were presented using E-prime system via a loudspeaker (Kurzweil KS-40A) placed in front of a child at a distance of 0.75 m.

EEG data were recorded at 128 electrode sites using Geodesic Sensor Nets (Electrical Geodesics, Inc., Eugene,OR, USA) with the operating impedance below 50 k $\Omega$ . The sampling rate was 1000 Hz. The electrode COM, placed next to the vertex (Cz) served as a common ground. Electrodes located at the edges of the cap, as well as bad channels, were excluded from the analysis. From the remaining electrodes 57 were selected to cover the entire head (7 electrodes at the midline and 25 electrodes placed over each hemisphere).

The data was downsampled offline to 250 Hz, band-passed filtered between 0.5-20 Hz and re-referenced to the mastoids (E57, E100). Epochs time-locked to the stimulus onset were extracted. The length of the epoch was 1100 ms, including a 100-ms prestimulus baseline. The artifact-contaminated epochs were automatically rejected if the amplitude of electrophysiological activity exceeded the absolute threshold of 120 mV. The eye movement artifacts were removed using the EEGLab implementation of ICA algorithm (runica [15]). The remaining epochs were then visually inspected to check for any other artifacts. Only standards immediately preceding deviants were included into the individual ERPs. In this way the number of trials for standards and deviants was kept equal for all ERP comparisons. The local negative peaks were defined within [500, 700] ms time window corresponding to the MMN. Peak amplitudes and latencies were extracted automatically at each electrode using the ERPLab Measurement Tool [16].

### B. Tensor generation

A fourth-order tensor  $\underline{Y} \in R_+^{I_f \times I_t \times I_c \times I_s}$  was constructed by performing time-frequency analysis (TFR) for all EEG channels of all subjects using epochs for two different stimuli (standard and one of deviant stimulus) to allow finding significant differences between their multi-domain signal signatures. The numbers of frequency bins ( $I_f$ ), time frames ( $I_t$ ),

channels ( $I_c$ ), and subjects ( $I_s$ ) provide the dimensions of the tensor.

In this study time-frequency analysis of ERPs is done using fixed time window lengths for all frequencies. The TFR was computed over a sliding time window for each trial and then averaged across trials. The whole trial interval is between  $[-100, 1000]$  ms and the time interval of interest is between  $[500, 700]$  ms. We have used a tapering window of 200 ms yielding 5 Hz freq resolution. The data analysis was performed using Fieldtrip software<sup>1</sup>.

### C. Nonnegative Tucker Decomposition (NTD)

The Tucker decomposition is a form of higher-order principal component analysis (PCA) [17]. It decomposes a tensor into a core tensor multiplied by a matrix along each mode. Given the  $N$ th-order tensor  $\underline{Y} \in R_+^{I_1 \times I_2 \times \dots \times I_N}$ , the NTD factorizes  $\underline{Y}$  as follows [11]:

$$\underline{Y} \approx \underline{G} \times_1 A^{(1)} \times_2 A^{(2)} \times_3 \dots \times_N A^{(N)} = \widehat{\underline{Y}}, \quad (1)$$

where  $\widehat{\underline{Y}}$  is an approximation of the tensor  $\underline{Y}$ , and  $A^{(n)} = [a_1^{(n)}, a_2^{(n)}, \dots, a_J^{(n)}] \in R_+^{I_n \times J_n}$  for  $n = 1, 2, \dots, N$  are the factor (component) matrices. The tensor  $\underline{G} \in R_+^{J_1 \times J_2 \times \dots \times J_N}$  is called the core tensor and its entries show the level of interaction between factor matrices, and  $\times_n$  represents the  $n$ -mode matrix product [11]. Note *en passant* that another frequently used tensor decomposition method, the CPD is a special case of Tucker decomposition whose core tensor is super-diagonal [11].

### D. Computing the Tucker decomposition

Determining the number of extracted components (columns) for each factor matrix (finding the size of the core tensor) is a crucial issue for efficient Tucker decomposition. In this study, we have used a triangle method [18], originally proposed for finding the location of the corner in the L-curve method. We are using the Tensorlab toolbox<sup>2</sup> mlrankst() function implementing the triangle method for estimation of the number of components in each factor matrix.

Most of NTD algorithms for obtaining Tucker decomposition are based on the minimization of the squared Euclidean distance (Frobenius norm) subject to the nonnegativity constraints as follows [10]:

$$D(\underline{Y}|\underline{G}, \{A\}) = \frac{1}{2} \|\underline{Y} - \underline{G} \times_1 A^{(1)} \times_2 A^{(2)} \times_3 \dots \times_N A^{(N)}\|_F^2. \quad (2)$$

At each iteration, the objective function is optimized with respect to a specific factor matrix  $A^{(n)}$ . The low speed convergence is the main bottleneck of this method due to the unfolding of tensor from one mode to another at each iteration. By considering NTD as a series of nonnegative matrix factorization (NMF) problems, we can accelerate the whole process. However, NMF algorithms may converge slowly on a large-scale problem. One solution is to use a low-rank approximation

method, such as PCA, to reduce dimensionality and speed up the convergence. Unfortunately, this method cannot be applied directly to nonnegative matrix factorization, as it usually violates the nonnegativity constraints. In this paper, we use the generalized version of low-rank approximation to NMF (IraNTF) algorithm to perform the nonnegative Tucker decomposition which is fast and robust to noise [19].

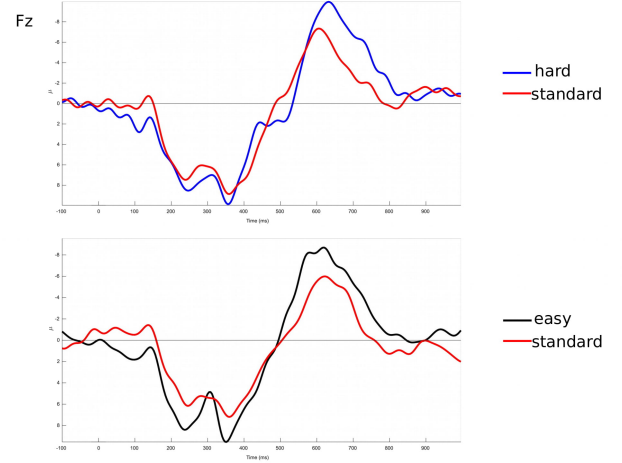


Fig. 2. The grand averaged responses to easy and hard deviants and corresponding standards

### E. Extracting the multi-domain features

A fourth-order tensor  $\underline{Y} \in R_+^{I_f \times I_t \times I_c \times I_s}$  was constructed to investigate the properties of ERPs in different domains simultaneously. Decomposition of  $\underline{Y}$  to extract the multi-domain features of ERPs is obtained using NTD as:

$$\underline{Y} \approx \underline{G} \times_1 A^{(f)} \times_2 A^{(t)} \times_3 A^{(c)}, \quad (3)$$

where  $A^{(f)} \in R_+^{I_f \times J_f}$ ,  $A^{(t)} \in R_+^{I_t \times J_t}$ ,  $A^{(c)} \in R_+^{I_c \times J_c}$ ,  $J_f$ ,  $J_t$ , and  $J_c$  are the numbers of extracted components for the spectral, temporal and spatial factors, respectively, and  $\underline{G} \in R_+^{J_f \times J_t \times J_c \times I_s}$  is the core tensor that carries the multi-domain features of ERPs. Note that the factor matrix for the subject dimension is an identity matrix of size  $I_s$  which allows for comparison of differences between two stimuli among the subjects based on coefficients of the core tensor. For example, given the spectral component  $j_f$ , the temporal component  $j_t$ , and the spatial component  $j_c$ , the multi-domain feature for subject  $i$  is obtained by  $G(j_f, j_t, j_c, i)$ . Hence, for each subject, there are exactly  $J_f \times J_t \times J_c$  multi-domain features.

## III. RESULTS

and discussion

### A. Conventional analysis

Fig. 2, demonstrates the grand averaged responses to easy and hard deviants and corresponding standards. Visual inspection of the figure reveals that there is a broad and heterogeneous positive deflection followed by a negative one

<sup>1</sup><http://www.ru.nl/neuroimaging/fieldtrip>

<sup>2</sup><https://www.tensorlab.net>

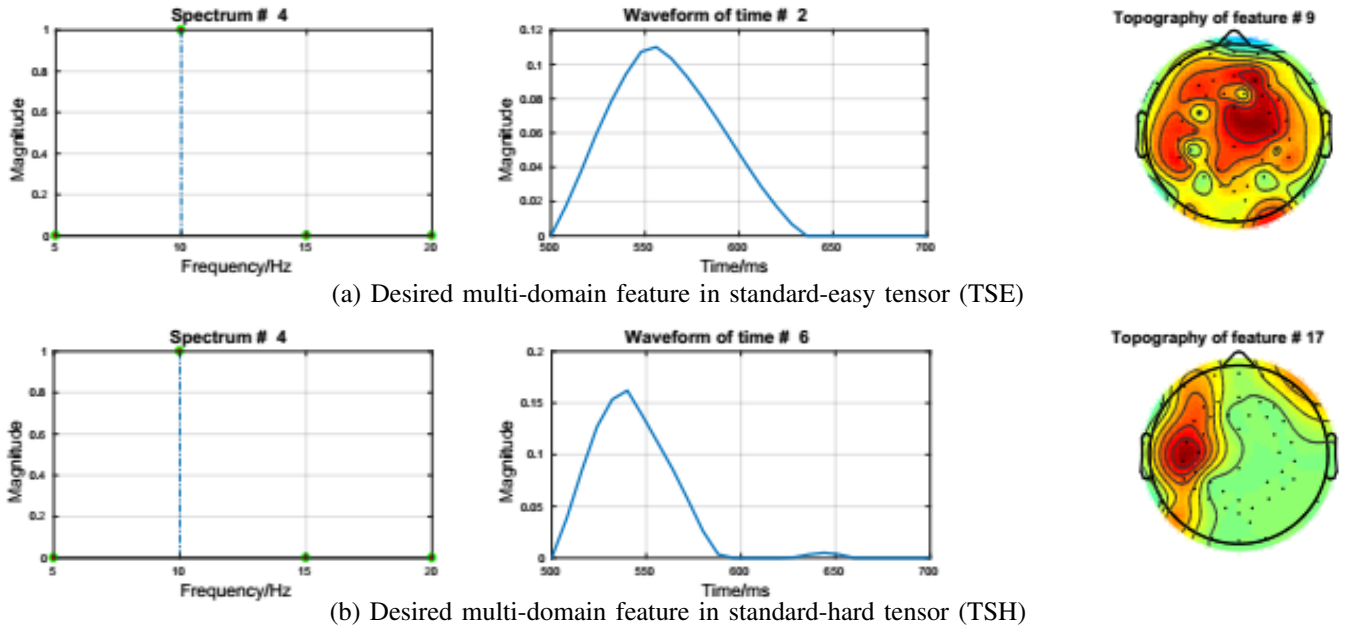


Fig. 3. Desired multi-domain features obtained from Nonnegative Tucker Decomposition.

that peaks around 550 ms, both in response to each deviant type and standard stimulus. The grand mean waveforms in our study are similar to those obtained in infants by other authors [20] [21]. Specifically, the response is biphasic with a large positive peak followed by the negative one. This shape of the waveform might be explained in terms of the immaturity of the auditory central nervous system. [22].

Although the negative peak in our study did not appear until about 500 ms after the stimulus and it was delayed compared to a conventional MMN response, which typically peaks around 200 ms [1], it still might represent MMN. This delay may be caused by complex and unusually long speech sounds that were used in our study (see: Fig.2) (in typical MMN experiments stimuli are about half the duration of the speech sounds applied here). The negative component in [500, 700] ms time window appeared also in response to standards, which is rather unusual for typical MMN experiments. On the one hand, an amplitude of this peak was still larger for deviants compared to standards suggesting the presence of MMN-like component. On the other hand, the positive component that preceded an MMN-like response was not uniform and it is possible to extract at least few subcomponents within it. Therefore, we might hypothesize that the heterogeneous positive and negative peaks form the complex of alternating auditory positive and negative components (P1-N1-P2-N2) that might be considered as ACC. This becomes even more likely when we take into account that in our study infants were exposed to relatively long and complex speech sounds. In this case ACC, which is considered as reflecting an acoustic change within the stimulus, should be expected [23]. Our results are partially in line with those demonstrated by [21] who aimed at testing the ACC elicited by long-duration speech

stimuli in infants. The authors found that ACC might be successfully used as an index of speech discrimination ability. However, contrary to our study, they did not use an oddball paradigm (infants listened to the stimuli presented randomly in a sequence). Since MMN is typically evoked by short stimuli in passive oddball protocols, whereas ACC appears in response to complex long-duration speech sounds, it is possible that in our study these two components overlapped. Further, it would be impossible to differentiate between MMN and ACC component based only on data analysis in the time domain. This is the reason why we decided to apply the tensor decomposition analysis enabling evaluation of temporal but also spatial and frequency characteristics of EEG signal.

### B. Multi-domain feature of MMN by NTD

Two fourth-order tensors: standard-easy (TSE) and standard-hard (TSH), with  $I_f = 4$  frequency bins,  $I_t = 26$  time frames,  $I_c = 57$  electrodes, and  $I_s = 42$  subjects were constructed for the standard vs. easy stimulus and standard vs. hard stimulus, respectively. Here, the first 21 coefficients in subjects' dimension represent results for the standard stimulus and the remaining 21 coefficients in subjects' dimension represent results for the easy deviant stimulus and the hard deviant stimulus in TSE and TSH, respectively.

Application of triangle method yields  $J_f = 4$  spectral components,  $J_t = 5$  temporal components,  $J_c = 20$  spatial components for TSE, and  $J_f = 4$  spectral components,  $J_t = 6$  temporal components,  $J_c = 21$  spatial components for TSH. The IraNTF algorithm produced stable NTD decomposition for such a setup. Due to lack of space, we omit the details of stability analysis in this report. One-way ANOVA (analysis of variance) tests were performed to find the multi-domain

feature(s) showing a significant difference between two stimuli for each tensor. Among such multi-domain features, the feature in Fig. 3(a) was selected as the desired multi-domain feature of MMN for TSE. The corresponding temporal component and the spectral component associated with the feature in Fig. 3(a) appears to match the properties of MMN in the time domain, i.e. the peak latency is around 550 ms, which is consistent with the data obtained in the conventional analysis (Fig. 2). The spatial domain, i.e. the fronto-central distribution of this peak also suggests that it is MMN response. On the other hand, the spectrum peaks at around 10 Hz whereas for a typical MMN the frequency band ranges below this value, from 2 to 8.5 Hz, would be more desired [24]. However, in the present study, due to time constraints of infant EEG experiments, the tensor analysis was performed in a relatively narrow time window  $[-100, 1000]$  ms which precluded fine-resolution spectral analysis, especially for low frequencies. Similarly, the desired feature of MMN for TSH is shown in Fig. 3(b). It has the desired temporal domain (the peak latency ca. 550 ms) and the same frequency domain (10 Hz) profiles than the feature presented in Fig. 3(a). TSH was distributed in the left auditory cortex which might suggest that it represents more ACC than MMN response.

In our study, we used two different types of deviants. One of them (easy) was chosen to be well discriminated from the standard stimuli. In this case, we expect to have the most apparent MMN response and our outcomes have shown that the TSE corresponded relatively well to MMN characteristics Fig. 3(a). The second deviant type (hard) is supposed to be difficult to differentiate by adult listeners but not necessarily by infants at the age of 8-12 months who, potentially, are capable to detect changes between all foreign phonemes [25]. Theoretically, then, in this group, MMN response to hard deviant might have occurred. However, we cannot exclude that hard deviant would be more difficult to distinguish from standards than the easy one also for infants and, thereby, elicit less pronounced MMN component. In this case, ACC might be more visible and have a greater contribution to MMN. ACC reflects any changes in the spectral properties of sounds and perhaps more precise analysis of hard stimulus by the analytical and speech-sensitive left auditory cortex is needed to differentiate this deviant type from the standard. Thus, it is possible that the feature presented in the Fig. 3(b), might correspond to ACC rather than MMN.

#### IV. CONCLUSIONS

The tensor analysis might be useful for detailed investigation of the overlapping components reflecting pre-attentive differentiation of speech sounds. This paper presents a relatively new methodological approach and the results should be interpreted with caution. Further analysis on a larger sample is needed to clarify the outcomes.

#### REFERENCES

- [1] R. Näätänen, P. Paavilainen, H. Titinen, D. Jiang, and K. Alho, "Attention and mismatch negativity," *Psychophysiology*, vol. 30, no. 5, pp. 436–450, 1993.
- [2] M. Rivera-Gaxiola, J. Silva-Pereyra, and P. K. Kuhl, "Brain potentials to native and non-native speech contrasts in 7- and 11-month-old American infants," *Developmental science*, vol. 8, no. 2, pp. 162–172, 2005.
- [3] M. I. Garrido, J. M. Kilner, K. E. Stephan, and K. J. Friston, "The mismatch negativity: a review of underlying mechanisms," *Clinical neurophysiology*, vol. 120, no. 3, pp. 453–463, 2009.
- [4] B. A. Martin and A. Boothroyd, "Cortical, auditory, evoked potentials in response to changes of spectrum and amplitude," *The Journal of the Acoustical Society of America*, vol. 107, no. 4, pp. 2155–2161, 2000.
- [5] J.-R. Kim, "Acoustic change complex: clinical implications," *Journal of Audiology Otology*, vol. 19, no. 3, p. 120124, 2015.
- [6] A. Cichocki, H. Lee, Y.-D. Kim, and S. Choi, "Non-negative matrix factorization with  $\alpha$ -divergence," *Pattern Recognition Letters*, vol. 29, no. 9, pp. 1433–1440, 2008.
- [7] T. M. Rutkowski, R. Zdunek, and A. Cichocki, "Multichannel EEG brain activity pattern analysis in time–frequency domain with nonnegative matrix factorization support," in *International Congress Series*, vol. 1301. Elsevier, 2007, pp. 266–269.
- [8] H. Lee, Y.-D. Kim, A. Cichocki, and S. Choi, "Nonnegative tensor factorization for continuous EEG classification," *International journal of neural systems*, vol. 17, no. 04, pp. 305–317, 2007.
- [9] S. Pouryazdian, A. Chang, D. J. Bosnyak, L. J. Trainor, S. Beheshti, and S. Krishnan, "Multi-domain feature selection in auditory Mismatch Negativity via PARAFAC-based template matching approach," in *Engineering in Medicine and Biology Society (EMBC), 2016 IEEE 38th Annual International Conference of the*. IEEE, 2016, pp. 1603–1607.
- [10] F. Cong, A.-H. Phan, P. Astikainen, Q. Zhao, Q. Wu, J. K. Hietanen, T. Ristaniemi, and A. Cichocki, "Multi-domain feature extraction for small event-related potentials through nonnegative multi-way array decomposition from low dense array EEG," *International journal of neural systems*, vol. 23, no. 02, p. 1350006, 2013.
- [11] T. G. Kolda and B. W. Bader, "Tensor decompositions and applications," *SIAM review*, vol. 51, no. 3, pp. 455–500, 2009.
- [12] A. Cichocki, D. Mandic, L. De Lathauwer, G. Zhou, Q. Zhao, C. Caiafa, and H. A. Phan, "Tensor decompositions for signal processing applications: From two-way to multiway component analysis," *IEEE Signal Processing Magazine*, vol. 32, no. 2, pp. 145–163, 2015.
- [13] F. Cong, A. H. Phan, H. Lyytinen, T. Ristaniemi, and A. Cichocki, "Classifying healthy children and children with attention deficit through features derived from sparse and nonnegative tensor factorization using event-related potential," in *International Conference on Latent Variable Analysis and Signal Separation*. Springer, 2010, pp. 620–628.
- [14] P. Boersma *et al.*, "Praat, a system for doing phonetics by computer," *Glott international*, vol. 5, 2002.
- [15] A. Delorme and S. Makeig, "EEGLAB: an open source toolbox for analysis of single-trial EEG dynamics including independent component analysis," *Journal of neuroscience methods*, vol. 134, no. 1, pp. 9–21, 2004.
- [16] J. Lopez-Calderon and S. J. Luck, "ERPLAB: an open-source toolbox for the analysis of event-related potentials," *Frontiers in human neuroscience*, vol. 8, p. 213, 2014.
- [17] I. Jolliffe, "Principal component analysis," in *International encyclopedia of statistical science*. Springer, 2011, pp. 1094–1096.
- [18] J. L. Castellanos, S. Gómez, and V. Guerra, "The triangle method for finding the corner of the L-curve," *Applied Numerical Mathematics*, vol. 43, no. 4, pp. 359–373, 2002.
- [19] G. Zhou, A. Cichocki, and S. Xie, "Fast nonnegative matrix/tensor factorization based on low-rank approximation," *IEEE Transactions on Signal Processing*, vol. 60, no. 6, pp. 2928–2940, 2012.
- [20] V. M. Little, D. G. Thomas, and M. R. Letterman, "Single-trial analyses of developmental trends in infant auditory event-related potentials," *Developmental Neuropsychology*, vol. 16, no. 3, pp. 455–478, 1999.
- [21] K. H. Chen and S. A. Small, "Elicitation of the acoustic change complex to long-duration speech stimuli in four-month-old infants," *International Journal of Otolaryngology*, vol. 2015, 2015.
- [22] A. Sharma, H. Glick, E. Deeves, and E. Duncan, "The P1 biomarker for assessing cortical maturation in pediatric hearing loss: a review," *Otorinolaringologia*, vol. 65, no. 4, p. 103, 2015.
- [23] B. A. Martin and A. Boothroyd, "Cortical, auditory, event-related potentials in response to periodic and aperiodic stimuli with the same spectral envelope," *Ear and hearing*, vol. 20, no. 1, pp. 33–44, 1999.
- [24] F. Cong, A. H. Phan, Q. Zhao, T. Huttunen-Scott, J. Kaartinen, T. Ristaniemi, H. Lyytinen, and A. Cichocki, "Benefits of multi-domain feature of mismatch negativity extracted by non-negative tensor factorization from EEG collected by low-density array," *International journal of neural systems*, vol. 22, no. 06, p. 1250025, 2012.
- [25] P. K. Kuhl, E. Stevens, A. Hayashi, T. Deguchi, S. Kiritani, and P. Iverson, "Infants show a facilitation effect for native language phonetic perception between 6 and 12 months," *Developmental science*, vol. 9, no. 2, pp. F13–F21, 2006.